HHS Public Access

Author manuscript

Toxicol Appl Pharmacol. Author manuscript; available in PMC 2015 December 31.

Published in final edited form as:

Toxicol Appl Pharmacol. 2014 July 15; 278(2): 135–147. doi:10.1016/j.taap.2014.04.019.

Interactive effects of cerium oxide and diesel exhaust nanoparticles on inducing pulmonary fibrosis

Jane Y.C. Ma[a,*], **Shih-Houng Young**[a], **Robert R. Mercer**[a], **Mark Barger**[a], **Diane Schwegler-Berry**[a], **Joseph K. Ma**[b], and **Vincent Castranova**[a]

[a]Health Effects Laboratory Division, National Institute for Occupational Safety and Health, Morgantown, WV 26505, USA

[b]School of Pharmacy, West Virginia University, Morgantown, WV 26506, USA

Abstract

Cerium compounds have been used as a fuel-borne catalyst to lower the generation of diesel exhaust particles (DEPs), but are emitted as cerium oxide nanoparticles (CeO_2) along with DEP in the diesel exhaust. The present study investigates the effects of the combined exposure to DEP and CeO_2 on the pulmonary system in a rat model. Specific pathogen-free male Sprague–Dawley rats were exposed to CeO_2 and/or DEP via a single intratracheal instillation and were sacrificed at various time points post-exposure. This investigation demonstrated that CeO_2 induces a sustained inflammatory response, whereas DEP elicits a switch of the pulmonary immune response from Th1 to Th2. Both CeO_2 and DEP activated AM and lymphocyte secretion of the proinflammatory cytokines IL-12 and IFN-γ respectively. However, only DEP enhanced the anti-inflammatory cytokine IL-10 production in response to ex vivo LPS or Concanavalin A challenge that was not affected by the presence of CeO_2, suggesting that DEP suppresses host defense capability by inducing the Th2 immunity. The micrographs of lymph nodes show that the particle clumps in DEP + CeO_2 were significantly larger than CeO_2 or DEP, exhibiting dense clumps continuous throughout the lymph nodes. Morphometric analysis demonstrates that the localization of collagen in the lung tissue after DEP + CeO_2 reflects the combination of DEP-exposure plus CeO_2-exposure. At 4 weeks post-exposure, the histological features demonstrated that CeO_2 induced lung phospholipidosis and fibrosis. DEP induced lung granulomas that were not significantly affected by the presence of CeO_2 in the combined exposure. Using CeO_2 as diesel fuel catalyst may cause health concerns.

Keywords

Cerium oxide; Diesel exhaust particles; Nanoparticle; Pulmonary inflammation; Lung fibrosis; Lymphatic system

[*]Corresponding author at: PPRB/HELD, NIOSH, 1095 Willowdale Road, Morgantown, WV 26505-2888, USA. Fax: +1 304 285 5938. jym1@cdc.gov (J.Y.C. Ma).

Conflict of interest

None.

Disclaimer: The findings and conclusions in this report have not been formally disseminated by the NIOSH and should not be construed to represent any agency determination or policy.

Introduction

Cerium, a member of the lanthanide series of metals, is the most abundant of the rare-earth elements in the Earth's crust (average concentration of 50 ppm) (Hedrick, 2004). Cerium oxide has been used commercially in polishing agents, television tubes, and precision optics and it is also applied in various consumer products including semiconductors (EPA, 2009). Recently cerium oxide has been used as a fuel borne catalyst in combination with a particulate filter in diesel engines to enhance combustion by reducing the ignition temperature of the carbonaceous particulate on the filter; thus, improving fuel burning efficiency and substantially decreasing particle mass in the exhaust. Recent studies demonstrated that cerium was generated in the diesel exhaust from an engine using standard diesel fuel spiked with either cerium oxide or suspension of "Envirox" (Cassee et al., 2012).

Diesel exhaust particles (DEPs) are carbon-based particles containing various organic compounds, including polycyclic aromatic hydrocarbons and nitroaromatic compounds adsorbed onto the carbonaceous core (Schuetzle, 1983; Schuetzle et al., 1981). Diesel exhaust is a complex and variable mixture of gases, vapors, and particulates containing numerous chemicals. Usage of diesel engines by various industries is increasing because of fuel efficiency. However, diesel engines emit 30–100 times more particulate matter (PM) than gasoline engines. The environmental health concerns for DEP stem from their substantial levels in urban and industrial areas as a major component of airborne PM, and the fact that epidemiological studies have demonstrated an association between exposures to PM and increased respiratory mortality and morbidity (Dockery et al., 1993).

Animal studies have shown that both the organic and the particulate components of DEP cause oxidant lung injury but trigger different cellular responses (Ma and Ma, 2002). Long-term exposure to DEP has been shown to induce tumor formation in rodents (Mauderly et al., 1987). Acute exposure to DEP induces pulmonary inflammation, activates alveolar macrophages (AMs), and alters the pulmonary immune/inflammatory responses to environmental allergens and bacterial infections (Dong et al., 2005; Yang et al., 1999, 2001; Yin et al., 2004). DEP is known to induce a change in pulmonary immune response that weakens the innate and cell-mediated immunity while enhances adaptive immune responses (Dong et al., 2005; Yin et al., 2004). Studies have shown that Th2 cytokines promote the differentiation of profibrogenic macrophages and the development of fibrotic diseases (Wynn, 2004).

With the addition of cerium in diesel fuel, the potential health effects associated with exposures to cerium oxide alone and in combination with DEP are not yet clear. This is consistent with the general consensus as to the high degree of uncertainty related to the environmental and health implications of manufactured-engineered nanomaterials (Cassee et al., 2011; Park et al., 2007; EPA, 2009). Cerium is known to induce rare earth pneumoconiosis characterized by accumulation of cerium particles (and other rare earth particles) in the lungs and lymphoreticular system after prolonged occupational exposure to cerium fumes or dust (Pairon et al., 1994, 1995; Porru et al., 2001; Sabbioni et al., 1982; Sulotto et al., 1986). Exposure was not quantified in any of these cases. The pathologic features of this rare earth pneumoconiosis include interstitial fibrosis, granulomas, and

bilateral nodular chest lesions. A common feature in this disease is the accumulation of cerium particles in the alveoli and interstitial tissue that persists even decades after exposure was ended (Pairon et al., 1994).

A previous study carried out in our laboratory demonstrated that exposure of rats to cerium oxide nanoparticles (CeO_2) by a single intratracheal instillation induced a sustained dose dependent pulmonary inflammatory response through 4 weeks post-exposure (Ma et al., 2011). At the end of 4 weeks, AM was transformed from the classic activated, inflammatory subset of M1 to the alternatively activated or fibrogenic subset M2, with a significant increase in arginase-1 expression (Ma et al., 2011). Pulmonary fibrosis was evident in the CeO_2-exposed lungs at 28 days post-exposure and the presence of CeO_2 in the lung tissue was demonstrated (Ma et al., 2011; Ma et al., 2012). These studies have also shown that the CeO_2 exposure not only increased production of the fibrotic cytokine, transforming growth factor (TGF)-β 1 and osteopontin (OPN), by AM, but also induced a range of mediators such as matrix metalloproteinases (MMPs), i.e., proteolytic enzymes involved in the degradation of extracellular matrix (ECM) collagens, and tissue inhibitor for MMP (TIMP), involved in the lung tissue remodeling. The imbalance of MMP-9/TIMP-1 may play an important role in the development of fibrosis.

Both CeO_2 and DEP caused severe lung injury. However, they exhibited different effects on pulmonary cellular responses. DEP exposure induced acute pulmonary inflammation that recovered with time, but a strong effect on lymphocyte differentiation that significantly suppressed the pulmonary self-defense capability against bacterial infection (Chan et al., 1981; Yin et al., 2002, 2003). In contrast, CeO_2 induced sustained inflammatory responses, which led to lung fibrosis. The presence of CeO_2 in diesel exhaust emissions, thus, may represent a serious occupational and environmental health risk with pulmonary fibrosis as a plausible end point. The objective of the current study is to characterize the effects of the presence of CeO_2 in DEP on pulmonary responses, including modification of DEP-induced cellular responses and lung fibrosis. Specifically, the present study investigates the combination exposure of DEP plus CeO_2 on lung inflammation and injury; lymphocyte responses and pulmonary defense capability; and development of fibrotic lung lesions.

Materials and methods

Materials

Specific pathogen-free male Sprague–Dawley (Hla:SD-CVF) rats (6 weeks old, ~200 g) were purchased from Hilltop Laboratories (Scottdale, PA). Rats were kept in cages individually ventilated with HEPA-filtered air, housed in an American Association for Accreditation of Laboratory Animal Care (AAALAC)-approved facility and provided food and water ad libitum. A standardized DEP sample (standard reference material 2975) was purchased from the National Institute of Standards and Technology (Gaithersburg, MD). Cerium oxide nanoparticles, 10 wt.% in water, were obtained from Sigma-Aldrich (St Louis, MO, USA).

Particle preparation

To prepare particle suspension, DEP, CeO_2 or DEP + CeO_2 was suspended in sterile saline then sonicated for 1 min using an ultrasonic processor (Heat System-Ultrasonics, Plainview, NY, USA). Particle suspension was prepared immediately before usage and was vigorously vortexed to provide well mixed suspension immediately before each instillation, it occurred less than 1 min later. In this practice, we did not experience the separation of the particles in the suspension. However, if one lets the suspension stand alone for some time the particles would separate out in the suspension. That was the reason for vortexing of the sonicated suspension.

Animal exposures

All rats were exposed and sacrificed according to a standardized experimental protocol that complied with the Guide for the Care and Use of Laboratory Animals and was approved by the National Institute for Occupational Safety and Health Animal Care and Use Committee. Animals were used after a 1 week acclimatization period. For particle exposure, rats were anesthetized with sodium methohexital (35 mg/kg, i.p.) and placed on an inclined restraint board. Rats were exposed to 0.3 ml suspensions of cerium oxide at a final concentration of 0.15, 0.5, 1, 3.5 or 7 mg/kg body weight, DEP (35 mg/kg), or CeO_2 + DEP via a single intratracheal instillation. Saline (0.9% NaCl) was administered to control rats. The treated animals (at least six in each treatment group) were sacrificed at 1, 3, 10 or 28 days post-exposure.

Particle characterization

The primary particle size and size of the particles as instilled have been characterized previously. The diameter of the primary CeO_2 particle is in the range of 6.4–14.8 nm with a mean of 9.26 ± 0.58 nm, determined by field emission scanning electron microscopy (FESEM). The diameter of primary particle was also determined to be in the range of 6.25–17.5 nm with a mean diameter of 10.14 ± 0.76 nm using transmission electron microscopy (TEM) (Nalabotu et al., 2011). We have also reported previously dynamic light scattering (DLS) of nanoparticles as diluted in saline for intratraceal instillation. These particles agglomerate in saline, with DLS showing a major particle peak at 2.5 μm and a small subpopulation with average size of 0.3 μm (Ma et al., 2011). The surface area of the particles used is in the range of 80–100 m^2/g using BET (Sigma Chemicals). The purity of the CeO_2 samples used in this study has been determined previously (Park et al., 2007; Yokel et al., 2009). The sum of the contamination from lead, aluminum, copper, titanium, iron, nickel and zinc was <0.2% of the Ce concentration according to ICP-MS analysis.

Isolation of bronchoalveolar lavage fluid and AM

Animals were anesthetized with sodium pentobarbital (0.2 g/kg, i.p.) and exsanguinated by cutting the renal artery. AM was obtained by bronchoalveolar lavage (BAL) with a Ca^{++} and Mg^{++}-free phosphate-buffered medium (145 mM NaCl, 5 mM KCl, 1.9 mM NaH_2PO_4, 9.35 mM Na_2HPO_4, and 5.5 mM glucose; pH 7.4) as described previously (Yang et al., 2001). Briefly, the lungs were lavaged with 6 ml Ca^{++} and Mg^{++}-free phosphate-buffered medium in and out twice for the first lavage, and subsequently lavaged with 8 ml of the same buffer

for a total of 10 times or when ~ total 80 ml BAL fluid (BALF) was collected from each rat. The acellular supernate from the first lavage was saved separately from subsequent lavages for further analysis. Cell pellets from each animal were combined, washed, and resuspended in a HEPES-buffered medium (145 mM NaCl, 5 mM KCl, 10 mM HEPES, 5.5 mM glucose, and 1.0 mM $CaCl_2$; pH 7.4). Cell counts and purity were measured using an electronic cell counter equipped with a cell sizing attachment (Coulter model Multisizer II with a 256C channelizer; Beckman Coulter, Fullerton, CA).

AM cultures

AM-enriched cells were obtained by adherence of lavaged cells to a tissue culture plate as described previously (Yang et al., 1999). AM was cultured in fresh Eagle minimum essential medium (EMEM, Lonza BioWhittaker, Walkersville, MD) containing 2 mM glutamine, 100 μg/ml streptomycin, 100 U/ml penicillin, 5 mM HEPES, and 10% heat-inactivated FBS (except for measuring TGF-β1 then only 1% heat-inactivated FBS was used) in the absence or presence of ex vivo lipopolysaccharide (LPS, 0.1 μg/ml) for an additional 24 h. AM-conditioned media were collected and centrifuged, and the supernates were saved in aliquots at −80 °C for further analysis of cytokines.

Lactate dehydrogenase (LDH), albumin content and chemiluminescence (CL)

The acellular LDH activity in the first BAL fluid was measured in fresh samples using Roche Diagnostic reagents and procedures (Roche Diagnostic Systems, Indianapolis, IN) on an automated Cobas C111 analyzer (Roche Diagnostic Systems). The albumin content in the first BAL fluid was measured based on albumin binding to bromocresol green with Roche Diagnostic reagents and procedures following the manufacturer's protocol.

Luminol-dependent CL, a measure of reactive oxygen species (ROS) formation, was monitored using a Berthold LB953 Luminometer (Berthold, Wildbad, Germany). CL generated by BAL cells (1×10^6 AM/ml) was measured before and after stimulation with unopsonized zymosan (2 mg/ml final concentration; Sigma Chemical Company, St. Louis, MO), a yeast cell wall that stimulates macrophages. The results were presented as total counts/15 min/10^6 AM. Zymosan-stimulated CL was calculated as the total counts in the presence of stimulant minus the corresponding basal counts as described by Park et al. (2007) and Yang et al. (2001).

Isolation of lung-associated lymphocyte, immunophenotyping and flow cytometry

Lung-associated lymph nodes were harvested, and suspended in 1 ml of EMEM without phenol red containing 2 mM glutamine, 100 μg/ml streptomycin, 100 U/ml penicillin, 5 mM HEPES and 10% heat-inactivated FBS (Sigma). Lymph nodes were gently homogenized using a tissue grinder with Teflon fluorocarbon resin and stainless-steel shaft pestle (Fisher Scientific, Pittsburgh, PA) to release lymphocytes into the medium. Total number of lymphocytes was determined using a Coulter Multisizer II.

Immunophenotyping was performed on lymphocyte suspensions via flow cytometry. Briefly, 100 μl of a blocking buffer containing 300 μg/ml mouse IgG was added to 50 μl of lymphocyte suspensions (~0.5×10^6 cells) for 10 min. Anti-CD3 and anti-CD45R were used

for T and B cell enumeration, respectively. 7-Aminoactinomycin D (7-AAD) and the monoclonal antibodies, anti-CD3, anti-CD4, anti-CD8a, anti-CD45R and NKR-P1A (Becton Dickinson, San Diego, CA) for different cell membrane surface markers, were prepared in FACS buffer (PBS with 0.2% BSA and 0.09% NaN_3) and added to above lymphocyte suspension for 30 min on ice. Samples were centrifuged and washed once with 1 ml FACS buffer to remove free antibody. The cells were then fixed with 1% paraformaldehyde (final concentration) and analyzed on FACSCalibur (Flow Cytomter, BD Biosciences Immunocytometry Systems, San Jose, CA). Two panels, each panel consists of 3 or 4 colors, were setup for immunophenotyping: CD45R-FITC/CD3-PE/7-AAD and CD4-FITC/NKR-P1A-PE/CD8-PerCP/CD3-APC. The viability of lymphocytes was identified by 7-AAD staining. The subsets of live lymphocytes were selected based on forward scatter and side scatter light signal intensity, which was set to exclude dead cells and contaminating red blood cells, which are smaller than live lymphocytes. A total of 10,000 events were collected for each sample. The absolute numbers of cells in each lymphocyte subpopulation were calculated by multiplying the total number of viable cells by the percentage of the total within each phenotype, determined by flow cytometry.

Lymphocytes (4×10^6/ml) were suspended in EMEM containing 2 mM glutamine, 100 μg/ml streptomycin, 100 U/ml penicillin, 5 mM HEPES, and 10% heat-inactivated FBS, and incubated in a humidified incubator (37 °C and 5% CO_2) for 24 h with or without Concanavalin A (ConA, 5.5 μg/ml) (Sigma Chemical Co.) as described preciously (Yin et al., 2003). The lymphocyte-conditioned media were collected and centrifuged (1200 × *g* for 4 min), and aliquots of the supernates were stored at −80 °C until assayed.

Measurement of soluble mediators, hydroxyproline, and phospholipids

IL-6, IL-10 and IFN-γ—The amounts of IL-6 and IL-10 produced by AM with or without ex vivo LPS challenge and IL-6, IL-10 and IFN-γ produced by lymphocytes with or without Concanavalin A (ConA) stimulation in cell culture medium were quantified by using the Cytometric Bead Array (CBA, BD Biosciences, Sparks, Maryland), bead-based immunoassays according to the manufacturer's instructions.

IL-12 and TGF-β1—IL-12 and TGF-β1 in AM-conditioned media were determined using enzyme-linked immunosorbent assays (ELISA), obtained from Biosource International, Inc. (Camarillo, CA) and from R&D Systems (Minneapolis, MN), respectively, according to the manufacturers' protocol.

Matrix metalloproteinase (MMP)-9 and tissue inhibitors of metalloproteinase (TIMP)-1—The levels of MMP-9 and TIMP-1 were determined in the first BALF, using ELISA kits from Cusabio Biotech Co., Ltd. (Wuhan, Hubei, China) and R&D Systems Inc. (Minneapolis, MN), respectively, following the manufactures' protocols.

Determination of MMP-9 activity—Electrophoresis was used to determine the gelatinase, MMP-9, activity in the first BALF. BALF samples of 15 μg of protein were loaded onto 10% Novex Zymogram (Gelatinase) gels (Life Technologies, Grand Island, NY), according to the manufacture's instruction. Briefly, after electrophoresis, gels were

incubate in renaturing buffer, washed with developing buffer and incubated with developing buffer overnight for maximum sensitivity. The gels were then stained in Coomassie brilliant blue and destained in methanol–acetic acid–water until clear bands of enzymatic activity were at optimal contrast from the blue staining gelatin background. Molecular weight standards were run on each gel. Gel intensity was determined using ImageQuant 5.1 (Life Technologies).

Phospholipids—Total phospholipids in BAL fluid were measured as the inorganic phosphorus present in the lipid extracts, which was extracted using chloroform–methanol (2:1, v/v) as described previously (Bartlett, 1959). Phospholipid content was obtained by multiplying lipid phosphorus values by 25 (Oyarzun and Clements, 1978).

Hydroxyproline determination—The formation of collagen in the lungs was analyzed by measurement of hydroxyproline content in the lung tissues. Rat lungs were chopped and hydrolyzed in 6 N HCl for 48–72 h at 110 °C. Hydroxyproline was determined according to the method of Witschi et al. (1985).

Transmission electron microscope (TEM) and field emission scanning electron microscopy (FESEM)—AM ultrastructure was analyzed by TEM. BAL cell pellets were fixed in Karnovsky's fixative (2.5% glutaraldehyde + 3% paraformaldehyde in 0.1 M sodium cacodylate, pH 7.4) and postfixed with osmium tetroxide. Cells were dehydrated in graded alcohol solutions and propylene oxide and embedded in LX-112 (Ladd, Williston, VT). Ultrathin sections were stained with uranyl acetate and lead citrate and examined with a TEM (JEOL 1220, Tokyo, Japan).

For FESEM, 8 μm thick paraffin sections were cut and deparaffinized. After sputter coating, the specimens were examined with a Hitachi Model S-4800 field emission scanning electron microscope at between 5 and 20 kV.

Histological examination—Rat lung tissues from different exposure groups were fixed immediately after sacrifice by intratracheal instillation of 10% neutral buffered formalin at a pressure of 30 cm H_2O (at an altitude of 960 ft), embedded in paraffin, and stained with hematoxylin and eosin for light microscopic examinations. The tracheobronchial lymph node at the base of the tracheal bifurcation was also removed, preserved by fixative and processed for observation by enhanced darkeld microscopy.

Enhanced darkfield imaging—CeO_2 and DEP particles were imaged in the lung tissue and lymph nodes using a high signal-to-noise, darkfield-based illumination on an Olympus BX-41 microscope (CytoViva, Auburn, AL) at 100× oil immersion. Nanoparticles, such as CeO_2 and DEP, have dimensions less than the wavelength of light, have closely packed atoms, and a refractive index significantly different from that of biologic tissues and/or mounting medium. These characteristics produce significantly greater scattering of light by nanoparticles than by the surrounding tissues. The enhanced-darkfield optical system images light scattered in the section and, thus, CeO_2 and DEP stand-out from the surrounding tissues with high contrast. For enhanced darkfield imaging, sections (5 μm thick) were

collected on ultrasonically cleaned, laser cut slides (Schott North America, Inc, Elmsford, N.Y. 10523) to avoid contamination from the ground edges of traditional slides.

Sirius Red staining for collagen detection—Collagen in the lungs was detected with Sirius Red staining (Junqueira et al., 1979), a quantitative morphometric method for collagen determination in the lungs (Antonini et al., 2000; Malkusch et al., 1995). Paraffin sections were deparaffinized and rehydrated with xylene–alcohol series to distilled water. The slides were then stained with 0.1% Picrosirius solution (100 mg of Sirius Red F3BA in 100 ml of saturated aqueous picric acid, pH 2) for 1–2 h, washed for 1 min in 0.01 N HCl, counterstained with Mayer's hematoxylin for 2 min, dehydrated, and mounted with a coverslip.

Quantitative morphometric analysis—Quantitative morphometric methods were used to measure the average thickness of the fibrillar collagen in the alveolar wall and the extent of collagen formation in the alveolar region, details were described previously (Ma et al., 2012). Volume and surface density were measured using standard morphometric analyses (Underwood, 1970), which consisted of basic point and intercept counting. Volume density was determined from counting the number of points over the appropriate structures in a section relative to total alveolar region points.

Statistical analysis—Data are presented as means ± standard errors. Comparisons were made using analysis of variance (ANOVA) with means testing by Dunnett's test to compare treatment groups to control or by Tukey–Kramer test to compare all groups. A $p \leq 0.05$ was considered to be significant.

Results

Particle characterization

Fig. 1 shows the micrographs of the samples of DEP, CeO_2, or their combination used in the exposures under FESEM. DEP particles exhibited typical clumps of material that were 38 ± 3 nm in diameter. The much smaller CeO_2 particles with a primary diameter of 8.3 ± 0.7 nm tended to form agglomerates. A sample of the combined DEP and CeO_2 particles used in exposures shows small clumps of CeO_2 on the larger DEP agglomerates. Deposition of DEP and CeO_2 agglomerates on the alveolar epithelial surface at 28 days post-exposure was also demonstrated. It is worth noting the results show that DEP and CeO_2 particles are co-localized. It appears that these two particles are together and not separated.

Particles induced inflammation, lung damage and ROS generation

At one day after exposure of rats to DEP (35 mg/kg), there was a significant increase influx of PMN, LDH activity and albumin leakage into air space, which are the markers for inflammation, cytotoxicity and air/capillary leakage, respectively (Fig. 2). DEP-induced inflammation and injury significantly declined to the control level at 28 days post-exposure, suggesting DEP-induced acute effects on lung inflammation and injury. In comparison, both CeO_2 and DEP + CeO_2 exposures significantly not only increased inflammation and injury at 1 day after exposure, but the effects also persisted throughout 28 days exposure period.

The inflammatory responses and lung damage caused by combined exposure of DEP + CeO_2 did not exceed the sum of the individual effects of DEP alone plus CeO_2 alone.

Both DEP and CeO_2 activated AM for ROS generation in response to zymosan stimulation measured by chemiluminescence (CL) generation at 1 day after exposure (Fig. 2D), which was signiflcantly reduced at 28 days post-exposure. At 1 day post-DEP + CeO_2-exposed AM-generated ROS was less than the sum of DEP alone and CeO_2 alone. However, at 28 days post-DEP + CeO_2-exposed AM generated ROS level similar to the sum of CL induced by the individual particle exposures.

Particle induced cytokine production by AM and acellular mediators

Exposure of rats to DEP or CeO_2, but not DEP + CeO_2, induced inflammatory cytokine IL-12 production by AM at 1 day after exposure (Fig. 3A), with or without ex vivo LPS challenge. The results also show that CeO_2-induced IL-12 secretion (6-fold of control) to a significantly greater extent than DEP-induced IL-12 at 2-fold of control.

Among all particle treatment groups, only DEP exposure induced production of IL-6 (Fig. 3B), a cytokine which plays a key role in lymphocyte proliferation and the switch of immune response from Th1 to Th2 as previously reported by Yin et al. (2003). However, in response to ex vivo LPS stimulation all particle-exposed AM secreted markedly elevated IL-6 at 40-, 34- and 10-fold of control for DEP-, DEP + CeO_2, and CeO_2, respectively. These results suggest that AMs were primed for altered immune responses, and that DEP played a role in eliciting a Th2 immunity.

Fig. 3C shows that none of the particle exposures induced anti-inflammatory cytokine, IL-10, secretion by resting AM. In contrast, after ex vivo LPS challenge, DEP-, and DEP + CeO_2, and CeO_2, -exposed AM produced significantly increased IL-10 at 27-, 20- and 6-fold of control, respectively. These results demonstrate that CeO_2 is the primary effector on AM production of IL-12. However, the production of IL-12, IL-10 and IL-6, after DEP + CeO_2 did not exceed the sum of DEP alone plus CeO_2 alone.

The temporal production of the fibrogenic cytokine, TGF-β1, by particle-exposed AM is shown in Fig. 3D. CeO_2- and DEP + CeO_2-exposed AM produced significantly higher levels of TGF-β1 than the control at 3 days post-exposure, and this increase was declined to the control level at 10 days post-exposure. DEP alone did not induce AM production of TGF-β1 or significantly affect CeO_2-induced TGF-β1 secretion.

The presence of MMP-9, a proteolytic enzyme, responsible for lung collagen degradation, and TIMP-1, an antiproteolytic enzyme that binds to MMP-9 to inactivate the enzyme, in the first BALF at 1 day after exposure is shown in Fig. 4. The results show that all particle exposure increased MMP-9 and TIMP-1 levels when compared to the controls, and there is a great excess of induced TIMP-1 compared to MMP-9. DEP-, DEP + CeO_2- or CeO_2-induced MMP-9 levels were 3.3-, 3.5 and 1.7-fold of the control, respectively, indicating that DEP and DEP + CeO_2 exposure induced significantly higher levels of MMP-9 than the CeO_2 group. However, the particle induced MMP-9 activity (Figs. 4C and D) was CeO_2 > DEP + CeO_2 > DEP with activity level at enhanced 8-, 4.5- and 2-fold of control,

respectively, with the control showing minimum activity. These results suggest that increased MMP-9 activity is primarily associated with CeO_2 exposure.

Effects of DEP and/or CeO_2 exposures on lymphocyte subpopulation in LDLN

The numbers of total lymphocytes and all the subpopulation of lymphocytes isolated from all exposure groups at 3 days post-exposure are given in Table 1. The results show that all particle exposures significantly increased total number of lymphocytes, T and T-cell subsets, NKT cells and B cells, when compared to the saline controls. CeO_2 induced total lymphocytes was significantly higher than the control, but lower than DEP-exposed groups. The $CD4^+/CD8^+$ ratio for all particle-exposed groups was significantly reduced in comparison to the control, which may attribute to a slightly reduced percentage of $CD4^+$ in total cells for the exposed groups (DEP, 51%; CeO_2, 50%; DEP + CeO_2, 53%; control, 59%) and a significant increase in the percentage of $CD8^+$ cells for the exposed groups (DEP, 40%; CeO_2, 42%; DEP + CeO_2-, 42%; control; 34%) as compared to the control. The increase in lymphocytes and T cell subsets by DEP + CeO_2 exposure is not markedly different from that of the DEP exposure, which is lower than the sum of individual particle effects, suggesting that CeO_2 has little effect on DEP-modulated lymphocyte proliferation.

Effects of DEP and CeO_2 exposures on lymphocyte cytokine production

The lymphocyte-mediated immune responses were assessed by monitoring cellular production of cytokines in response to ConA stimulation. Fig. 5 shows that lymphocytes were primed by all particle exposures, DEP, CeO_2, and DEP + CeO_2, to produce significantly elevated IFN-γ production in response to ConA stimulation. However, ConA-stimulated IL-10 production was only associated with DEP-and DEP + CeO_2-, but not CeO_2-exposed groups. These results suggest that both DEP and CeO_2 induced lymphocyte production of the inflammatory cytokine (IFN-γ), whereas DEP plays major role in activating anti-inflammatory responses in lymphocyte (IL-10).

Phospholipidosis characterization

TEM shows that numerous vacuoles and lamella bodies were detected in AM isolated from rats exposed to DEP (35 mg/kg) + CeO_2 (3.5 mg/kg)- and CeO_2-exposed AM, but not DEP at 10 days post-exposure (Fig. 6). The phospholipid (PL) content in the BAL fluid of DEP-exposed lungs was not significantly different from the saline control. However, there was a significant increase of PL in the DEP + CeO_2-and CeO_2-exposed lung when compared to the controls at 28 days postexposure, suggesting that CeO_2 is responsible for accumulation of phospholipids in the lung.

The presence of particles in the lung and lymph nodes

The distribution of particles within the lung tissues was readily demonstrated using the enhanced darkfield imaging system. At 28 days after exposure of rats to CeO_2 or DEP + CeO_2, illuminated CeO_2 particles were detected mainly in AM, the interstitium and in the airspace as clumps mixed with phospholipids of lung surfactant. No particles were detected in control lung tissues (Fig. 7A). Fig. 7B shows the stained (H&E) sections of the tracheobronchial lymph nodes in saline, CeO_2-, DEP + CeO_2- and DEP-exposed lungs.

CeO_2 was distributed in clumped regions approximately 10–15 μm diameter in the lymph nodes of CeO_2 exposed lungs. DEP particles in the lymph nodes of DEP only exposed lungs were generally found in isolated dense clumps approximately 2 μm in diameter. As illustrated in Fig. 7B, the particles in the lymph nodes of DEP + CeO_2 exposed lungs were substantially greater than either the CeO_2- or DEP-exposed lungs with dense clumps being nearly continuous throughout the lymph node.

Pulmonary fibrosis

Hydroxyproline content, a specific marker for collagen, was determined in the lung tissues collected at 28 days post-exposure to DEP (35 mg/kg) in the absence or presence of CeO_2 (7 mg/kg) as shown in Fig. 8A. The results show a significant increase in pulmonary hydroxyproline content in rats exposed to DEP, CeO_2 or DEP + CeO_2.

Histopathological analysis showed that the light micrographs of DEP (35 mg/kg)-exposed lungs, at 28 days post-exposure demonstrate granulomatous lesions with some collagen fiber (Fig. 8B), whereas CeO_2 (7 mg/kg)-exposed lungs exhibited large acellular clumps of material (open arrow) with significant alveolar interstitial collagen formation (arrow). Fig. 8B shows that the granulomatous lesions of DEP-exposed lungs have far less collagen, fewer cells, and the DEP particles are much more densely distributed when compared to DEP + CeO_2-exposed lungs. The granulomatous tissue formation was 7.9 ± 2.4% and 9.7 ± 3.1% of all alveolar tissue volume in DEP and DEP + CeO_2 groups, respectively. Quantitative morphometric analysis of the average thickness of the alveolar wall and the extent of collagen formation showed that the alveolar wall thickness (Fig. 8C), excluding additional tissue formation in areas of granulomatous lesions, was significantly increased in the DEP, CeO_2, and DEP + CeO_2 groups by 20, 22, and 26%, respectively, over the controls.

In detecting alveolar collagen formation via Sirius Red staining, histological analysis shows significant elevated level of collagen in CeO_2-, DEP- or DEP + CeO_2-exposed lungs. The alveolar wall collagen fiber volume was increased by more than two fold over the control (Fig. 8D), suggesting that both DEP (at high exposure doses) and CeO_2 are fibrotic agents. The collagen level after DEP + CeO_2 was approximately the sum of the individual exposure.

Discussion

Exposure to DEP has been shown to cause acute lung inflammation and exacerbate the innate and cell-mediated immune responses to bacterial infection in short term exposures (Harrod et al., 2005; Yin et al., 2003). Previously, we have also demonstrated that CeO_2 nanoparticles induce a sustained inflammatory response which leads to pulmonary fibrosis (Ma et al., 2011, 2012; Park et al., 2007). Exposure to the combination of DEP and CeO_2 can result from using fuel additives containing cerium, since generated CeO_2 nanoparticles in exhaust have been reported. Thus, exposure to DEP + CeO_2 presents a complex and largely unknown health concern. The present study was carried out to examine the effects of the mixture of DEP and CeO_2 exposure on lung injury and the development of pulmonary diseases.

Exposure of rats to 35 mg/kg DEP seems a high concentration, however, in the rat 35 mg/kg DEP would be 8.7 mg/rat lung. The alveolar epithelial surface area of a human lung is 102 m^2, while that of the rat is 0.4 m^2 (Stone et al., 1992). Therefore, the alveolar surface area of the human lung is 255 times than that of the rat and an equivalent lung burden in a human would be 2.2 g/lung. According to the EPA estimates, the mean air concentration of DEP nationwide is 2.6 μg/ml. But in certain non-occupational settings such as in bus stops, the air concentration can be considerably higher. In fact, in the Los Angeles Basin, one estimate has placed the rate of DEP intake at 300 μg per 1–3 days (Diaz-Sanchez, 1997). Using a 25% deposition rate for humans, one can arrive at a value of 75 μg for the daily deposit. However, in the occupational settings, the air concentration of DEP can be considerably higher. The Department of Labor reported, as high as 2–3 mg/m^3 of DEP were found in underground mining operations. Using a minute ventilation value of 20 l/min, a 25% deposition for human (Valberg and Watson, 1996), and an air concentration of 1 mg/m^3, the daily (8-hour exposure) deposit of DEP would be 2400 μg. Therefore, a lung burden of 2.2 g could be attained in 3.6 years of underground mining in operations using diesel engines. We would like to point out, that the DEP dose used in the current study yielded lung deposits that is within the range of possible DEP intake.

The projected human pulmonary dose for inhalation of CeO_2 in diesel exhaust from engines using a CeO_2 fuel additive is 0.09 μg/kg body weight for 8 h (Health Effects Institute [HEI], 2001). CeO_2 is insoluble particle, and studies have shown that the clearance of CeO_2 from the lung may take 20 years or more (Pairon et al., 1994). As a diesel exhaust product, it is likely that the potential exposure to CeO_2 is continuous and the lung burden is cumulative.

A limited number of short-term diesel engine tests have confirmed that cerium (20 to 100 ppm in the fuel) used with the particulate filter substantially decreases both particle mass (>90%) and number (99%) concentrations in the exhaust (HEI, 2001). Despite the filter's high efficiency in trapping particulate matter (PM), however, a small amount of cerium is emitted in the particulate phase of the exhaust and mainly in the oxide form and in particles less than 0.5 μm in diameter. Cerium mass relative to the total particle mass was between 3% and 18% based on two tests using two different types of filters. According to HEI (2001) report, doses of CeO_2 were chosen at 3, 10 or to 20% of DEP in the present study.

In the present study, as demonstrated by FESEM, small clumps of CeO_2 on the larger DEP agglomerates were identified in lungs after mixed particle exposure. The persistence of particles in the lung was demonstrated, since DEP and CeO_2 agglomerate were detected on alveolar epithelial surface of the DEP + CeO_2-exposed lungs at 28 days post-exposure.

The localization of CeO_2 in the lung tissues, at 28 days post-exposure, as the dark field illuminated CeO_2 particles was detected in AM, the interstitium, and the airspace that was mixed with lung surfactant of DEP + CeO_2- and CeO_2-exposed lungs. These results show that DEP and CeO_2 are co-localized in the lung tissues and may direct stimulation of cells by both particles.

The dark field illuminated CeO_2 particles were also detected in the lymph nodes, at 28 days post-exposure; suggesting translocation of the particles from the alveolar region into the

local lymphoid system. Similar translocation of DEP from the lungs to lymph nodes was also observed and has been previously reported (Chan et al., 1981; Yu and Yoon, 1991), indicating that lymphatic system was involved in the removal of these particles from the pulmonary airways. Studies have shown that occupational exposure of workers for many years to rare earth-containing fumes and/or dusts resulted in high rare earth concentrations in the worker's pulmonary and lymph node systems. These particles were detected in the worker's lung even at about two decades after their retirement from work (Sulotto et al., 1986), and resulted in the development of pulmonary fibrosis (Gong, 1996; McDonald et al., 1995; Vocaturo et al., 1983; Waring and Watling, 1990). The findings from our studies demonstrate that particles exist in the lung and lymph nodes after a single intratracheal instillation of DEP and/or CeO_2 particles, which parallel the findings of the rare earth dust in the workers' lung.

Direct stimulatory effects of DEP and CeO_2 on cellular responses have been demonstrated as activation of cell secretion of pro- and anti-inflammatory cytokines. Exposure to DEP has been shown to increase the susceptibility of the lung to bacterial infection in rats (Ma et al., 2012; Yang et al., 2001; Yin et al., 2002) through enhanced AM production of anti-inflammatory cytokine, IL-10, which prolongs bacteria survival in AM (Ma et al., 2012; Yang et al., 1999; Yin et al., 2002, 2005, 2007). The present study shows that DEP stimulated AM production of IL-12 and IL-6, which is known to induce B-cell differentiation, regulates the acute-phase responses to injury (Kishimoto, 2005; Mihara et al., 2012) and the activation of T cells (Lotz et al. 1988). In addition, DEP also stimulated AM production of IL-10 in response to ex vivo LPS stimulation. On the other hand, lower concentration of CeO_2 up-regulates IL-12 production by AM, both at basal or in response to ex vivo LPS challenge, is significantly higher than DEP, and suggests that CeO_2 plays a major role in particle-induced inflammation. The gross effects of these particles are such that DEP causes a switch of the pulmonary immune response from Th1 to Th2, while CeO_2 induces a sustained inflammatory response in the lungs, switching AM function from the classical inflammatory subset M1 to the fibrotic subset of M2 at 4 weeks exposure time (Ma et al., 2011; Park et al., 2007). In the mixed exposures to DEP and CeO_2, where both particles are co-localized, the present study shows that exposure of rats to DEP and/or CeO_2 at 1 day post-exposure significantly increased proinflammatory cytokine, IL-12, production by AM basally or in response to ex vivo LPS stimulation in the following potency order: $CeO_2 \gg$DEP > DEP + CeO_2 ~ control. These findings suggest that DEP + CeO_2 exposure induced lung inflammation is in much reduced level when compared to CeO_2-exposed rats. In contrast, particle-exposed AM when challenged with ex vivo LPS, significantly increased anti-inflammatory cytokine, IL-10, secretion in potency orders of DEP ~ DEP + CeO_2 $\gg CeO_2$ ~ control. These results demonstrated that the combined exposure induced anti-inflammatory response is similar to DEP-induced effects, which is much higher than CeO_2. These findings clearly demonstrate that CeO_2 is a major effector for the inflammatory responses in the lung, while DEP, but not CeO_2, dominates the induction of anti-inflammatory cytokine production in response to LPS challenge. These findings show that the combined particle exposure diminished any single particle-induced inflammatory cytokine production, but that anti-inflammatory cytokine secretion is similar to the DEP level.

While DEP strongly modulated the immune responses in the lung, the effects of CeO_2 on the pulmonary immune system have not been investigated in detail. The present study showed that DEP and DEP + CeO_2 exposures induced a 4-fold increase in total lymphocyte counts in comparison to the controls. CeO_2 exposure alone resulted in a two-fold induction of pulmonary lymphocytes, suggesting that DEP is the major effector for lymph nodes immune responses in the mixed particle exposure. The increase in lymphocytes by CeO_2 and/or DEP was characterized by an increase in CD4+ and CD8+ cells and a decrease in the CD4+/CD8+ ratio to ~70% of the control, which may due to a greater increase in CD8+ than CD4+ cells. Our study further showed that CeO_2 and DEP induced different lymphocyte populations. Lymphocytes from all particle exposure groups in response to ConA stimulation produced increased IFN-γ to the similar level, but the production of IL-10 by lymphocytes was only associated with DEP with or without the presence of CeO_2, but not with CeO_2 exposure alone. This suggests that, CeO_2 induces a Th1 type cell response, whereas DEP-induced not only Th1 but also Th2 type responses. Studies by Park et al. (2009) have shown that exposure of mice to CeO_2 at a relative high concentration (50 mg/kg) by intratracheal instillation induced inflammatory responses, activated AM, and stimulated naïve T cells to trigger an adaptive immune response. They showed that CeO_2 exposure induced both Th1-type cytokine (IFN-γ and IL-12) and Th2-type cytokine (IL-4, IL-5 and IL-10) productions. The high yield of Th2-type cytokines from that study contrasts with the results of the current investigation may be due to a difference in animal species and/or exposure dose. For the cytokine measurement, our studies were carried out at an intratracheal dose of 3.5 mg/kg of CeO_2 when compared to 50 mg/kg dose used by Parker et al. (2009).

One of the major effects of CeO_2 on the exposed lung is the induction of phospholipidosis prior to the development of pulmonary fibrosis. Our studies demonstrated that the accumulation of lung surfactant, as measured BAL phospholipids, occurs in the lungs of DEP + CeO_2- and CeO_2-, but not DEP-exposed rats. TEM analysis further illustrated increased surfactant in the lung as vacuoles and lamellar bodies in and around AM from DEP + CeO_2- and CeO_2-exposed lungs, that is clearly absent in DEP-exposed lungs.

MMP-9 and TIMP-1 represent the proteolytic and antiproteolytic enzymes that control the balance between ECM synthesis and degradation of matrix components that is crucial for tissue repair (Gueders et al., 2006). MMPs were characterized by their extensive ability to degrade ECM proteins including collagens. However, in vivo activity of MMPs is generally very low and their transcription is tightly regulated by cytokines including IL-6 and growth factors such as TGF-β (Birrell et al., 2006; Papakonstantinou et al., 2003). MMPs can proteolytically activate or inactivate these cytokines, in addition some active MMPs can activate other proMMPs. However, activated MMPs are further regulated by endogenous inhibitors, TIMPs. In general, the concentrations of TIMPs far exceed MMPs in tissue and extracellular fiuids to limit MMP proteolytic activity to focal pericellular sites. The present study shows that all particle exposure significantly induced MMP-9 and TIMP-1 level with a potency of DEP ~ DEP + CeO_2 > CeO_2 in the first BALF collected at 1 day post-exposure. DEP-, DEP + CeO_2- or CeO_2-induced MMP-9 level by 3.3-, 3.5 and 1.7-fold of control, demonstrated that DEP and DEP + CeO_2 exposure induced significantly higher level of MMP-9 than CeO_2 group. In contrast, these same exposures induced MMP-9 activity were

in the following decreasing order: $CeO_2 \gg$DEP + CeO_2 > DEP at 91-, 18- and 7-fold increase, respectively, when compared to the controls. These data show exposure of animals to CeO_2 induced 2-fold increase of MMP-9 level but with 91-fold increase of its activity, suggesting that CeO_2-induced most MMP-9 activity in the lung when compared to DEP- or DEP + CeO_2-exposed lungs. Thus, CeO_2 is the major particle responsible for fibrotic lung lesions. Indeed, previously, we have reported that exposure of rats to a single intratracheal instillation of CeO_2 induced pulmonary fibrosis in a dose- and time- dependent manner (Ma et al., 2012), and involved enhanced levels of MMP-9 and TIMP-1 in the exposed lungs.

The histopathological features of the lung tissues from DEP + CeO_2-exposed animals are significantly different from any single particle, DEP- or CeO_2-exposed rats. Exposure of rats to DEP or DEP + CeO_2, but not CeO_2, produced aggregations of inflammatory cells (principally macrophages), interstitial cells and collagen fibers in the lungs to form granulomatous lesions. At 4 weeks after exposure these granulomatous masses generally walled off the DEP or DEP + CeO_2 particles in the lungs, suggesting that DEP is the particle responsible for lung granulomas. Although, CeO_2 in the combined exposure did not significantly affect DEP-induced lung granuloma, it led to significant accumulation of surfactant in the lung. CeO_2- or DEP + CeO_2-, but not DEP-induced fibrosis is accompanied by a significant accumulation of surfactant, as revealed by TEM micrographs and manifested by largely increased number of vacuoles and lamellar bodies in and around AM in the alveolar spaces. The present study demonstrates that the presence of CeO_2 in DEP exposure significantly modified DEP-induced lung morphology leading to phospholipidosis and lung fibrosis, but did not significantly affect DEP-induced lung granulomas.

Histological analysis has also shown that DEP detected in DEP-exposed lungs, was much denser than DEP found in the DEP + CeO_2-exposed lungs. These results were consistent with the fact that considerably more DEP was removed by bronchoalveolar lavage from the combined particle exposure than from DEP-exposed lungs. The reason for the better removal of DEP from the lung in the presence of CeO_2 is not clear at the present time. However, CeO_2 induced accumulation of surfactant, which has been shown to decrease the agglomeration of nanoparticles (Vaisman et al., 2006). Thus, this increased surfactant may play a role as dispersing agent for DEP accelerating the removal rate of these particles.

CeO_2 is the major effector for increasing collagen in the lungs after the combined exposure, since significantly increased pulmonary hydroxyproline content, a major component of collagen, was detected in CeO_2- and DEP + CeO_2-, but not DEP-exposed lungs. This is consistent with previous findings that CeO_2 increased lung collagen formation in a dose- and time-dependent manner in a rat model (Ma et al., 2012). Morphometric analysis further demonstrated that the alveolar wall localization of collagen in DEP + CeO_2-exposed lung tissues was similar to that in CeO_2-exposed lungs.

In summary, CeO_2 strongly induces lung collagen formation, excessive accumulation of lung surfactants, and cellular mediators involved in the lung tissue remodeling process that are not significantly affected by the presence of DEP. In addition, the presence of CeO_2 did not markedly affect DEP-induced lung granuloma. However, the present study shows that CeO_2 and DEP exhibit diverse effects on AM and pulmonary lymphocytes. DEP elicits a

cellular response characterized by granulomas and enhanced production of anti-inflammatory cytokines by AM and lymphocytes and weakened host defense against bacterial LPS challenge. In contrast, CeO_2 strongly induces sustained cellular production of inflammatory and fibrotic cytokines and accumulation of lung surfactant and fibrosis. There is strong evidence, however, that these particles, through combined exposure, are co-localized in the lung tissues and are able to elicit multiple responses from lung cells, leading to the development of lung injury, granulomas, impairment of cell-mediated immunity, and pulmonary fibrosis. This study has also demonstrated that any single particle exposure, CeO_2 or DEP, induced inflammatory responses in the lung, whereas in the combined exposure, DEP + CeO_2, which did not lead to lung inflammation, demonstrate that the combined exposure to DEP + CeO_2 exhibited features that cannot be readily predicted by results from either single particle exposure, suggesting more studies are warranted regarding the combined effects of DEP and CeO_2 on the pulmonary system.

Conclusion

This study shows that CeO_2 and DEP nanoparticles induce lung injury and co-localized in the lung tissues after combined exposure. CeO_2 induced sustained inflammation and surfactant accumulation, and altered the balance of mediators involved in tissue repair process leading to excess collagen deposit and pulmonary fibrosis. DEP induced acute inflammation, activated anti-inflammatory cytokine production by lung cells and suppressed the pulmonary defense capability in response to bacterial challenge. However, pulmonary responses to the combined exposure of DEP + CeO2 cannot be readily predicted by results from either single particle exposure, indicating that CeO_2 generated in exhaust emission with DEP from diesel engine using cerium fuel additive may pose serious adverse health effects. Future studies to elucidate the mechanisms of these toxicological responses to CeO_2 and DEP exposure are warranted.

Acknowledgments

We thank Ms. Lori Battelli and Mr. Dean Newcomer for contributions to the pathological analysis work in this paper.

Abbreviations

AM	alveolar macrophage
Arg-1	arginase-1
BAL	bronchial alveolar lavage
CeO_2	cerium oxide
ConA	Concanavalin A
DEP	diesel exhaust particle
ECM	extra-cellular matrix
EMT	epithelial–mesenchymal transition

IPF	idiopathic pulmonary fibrosis
MMP	matrix metalloproteinase
OPN	osteopontin
PM	particulate matter
PL	phospholipids
RE	rare earth
ROS	reactive oxygen species
TGF	transforming growth factor
TIMP	tissue inhibitors of matrix metalloproteinase
TEM	transmission electron microscopy

References

Antonini JM, Hemenway DR, Davis GS. Quantitative image analysis of lung connective tissue in murine silicosis. Exp Lung Res. 2000; 26:71–88. [PubMed: 10742923]

Bartlett GR. Phosphorus assay in column chromatography. J Biol Chem. 1959; 234:466–468. [PubMed: 13641241]

Birrell MA, Wong S, Dekkak A, De AJ, Haj-Yahia S, Belvisi MG. Role of matrix metalloproteinases in the inflammatory response in human airway cell-based assays and in rodent models of airway disease. J Pharmacol Exp Ther. 2006; 318:741–750. [PubMed: 16690722]

Cassee FR, van Balen EC, Singh C, Green D, Muijser H, Weinstein J, et al. Exposure, health and ecological effects review of engineered nanoscale cerium and cerium oxide associated with its use as a fuel additive. Crit Rev Toxicol. 2011; 41:213–229. [PubMed: 21244219]

Cassee FR, Campbell A, Boere AJ, McLean SG, Duffin R, Krystek P, et al. The biological effects of subacute inhalation of diesel exhaust following addition of cerium oxide nanoparticles in atherosclerosis-prone mice. Environ Res. 2012; 115:1–10. [PubMed: 22507957]

Chan TL, Lee PS, Hering WE. Deposition and clearance of inhaled diesel exhaust particles in the respiratory tract of Fischer rats. J Appl Toxicol. 1981; 1(2):77–82. [PubMed: 6206117]

Diaz-Sanchez D. The role of diesel exhaust particles and their associated polyaromatic hydrocarbons in the induction of allergic airway disease. Allergy. 1997; 52:52–56. Review, 16 refs. [PubMed: 9208060]

Dockery DW, Pope CA III, Xu X, Spengler JD, Ware JH, Fay ME, et al. An association between air pollution and mortality in six U.S. cities. N Engl J Med. 1993; 329:1753–1759. [PubMed: 8179653]

Dong CC, Yin XJ, Ma JYC, Millecchia L, Wu ZX, Barger MW, et al. Effect of diesel exhaust particles on allergic reactions and airway responsiveness in ovalbumin-sensitized brown Norway rats. Toxicol Sci. 2005; 88:202–212. [PubMed: 16107553]

EPA, U.S. Toxicological Review of Cerium Oxide and Cerium Compounds. 2009. EPA/635/R-08/002F. http://www.epa.gov/iris/toxreviews/1018tr.pdf

Gong H Jr. Uncommon causes of occupational interstitial lung diseases. Curr Opin Pulm Med. 1996; 2:405–411. [PubMed: 9363175]

Gueders MM, Foidart JM, Noel A, Cataldo DD. Matrix metalloproteinases (MMPs) and tissue inhibitors of MMPs in the respiratory tract: potential implications in asthma and other lung diseases. Eur J Pharmacol. 2006; 533:133–144. [PubMed: 16487964]

Harrod KS, Jaramillo RJ, Berger JA, Gigliotti AP, Seilkop SK, Reed MD. Inhaled diesel engine emissions reduce bacterial clearance and exacerbate lung disease to *Pseudomonas aeruginosa* infection in vivo. Toxicol Sci. 2005; 83:155–165. [PubMed: 15483187]

Health Effects Institute (HEI). Evaluation of human health risk from cerium added to diesel fuel. In: Hibbs, JB., Jr, editor. HEI Communication. Vol. 9. Boston, MA, USA: 2001.

Hedrick, JB. US Geological Survey. Vol. I. U.S. Department of the Interior; Reston, VA: 2004. Rare earths. Minerals yearbook. Metals and minerals. Available online at http://minerals.usgs.gov/minerals/pubs/commodity/myb/

Junqueira LC, Bignolas G, Brentani RR. Picrosirius staining plus polarization microscopy, a specific method for collagen detection in tissue sections. Histochem J. 1979; 11:447–455. [PubMed: 91593]

Kishimoto T. IL-6: from laboratory to bedside. Clin Rev Allergy Immunol. 2005; 28:177–186. [PubMed: 16129902]

Lotz M, Jirik F, Kabouridis P, Tsoukas C, Hirano T, Kishimoto T, et al. B cell stimulating factor 2/interleukin 6 is a costimulant for human thymocytes and T lymphocytes. J Exp Med. 1988; 167:1253–1258. [PubMed: 3127525]

Ma JY, Ma JK. The dual effect of the particulate and organic components of diesel exhaust particles on the alteration of pulmonary immune/inflammatory responses and metabolic enzymes. [Review] [121 refs]. J Environ Sci Health C Environ Carcinog Ecotoxicol Rev. 2002; 20:117–147. [PubMed: 12515672]

Ma JY, Zhao H, Mercer RR, Barger M, Rao M, Meighan T, et al. Cerium oxide nanoparticle-induced pulmonary inflammation and alveolar macrophage functional change in rats. Nanotoxicology. 2011; 5:312–325. [PubMed: 20925443]

Ma JY, Mercer RR, Barger M, Schwegler-Berry D, Scabilloni J, Ma JK, et al. Induction of pulmonary fibrosis by cerium oxide nanoparticles. Toxicol Appl Pharmacol. 2012; 262:255–264. [PubMed: 22613087]

Malkusch W, Rehn B, Bruch J. Advantages of Sirius Red staining for quantitative morphometric collagen measurements in lungs. Exp Lung Res. 1995; 21:67–77. [PubMed: 7537210]

Mauderly JL, Jones RK, Griffith WC, Henderson RF, McClellan RO. Diesel exhaust is a pulmonary carcinogen in rats exposed chronically by inhalation. Fundam Appl Toxicol. 1987; 9:208–221. [PubMed: 2443412]

McDonald JW, Ghio AJ, Sheehan CE, Bernhardt PF, Roggli VL. Rare earth (cerium oxide) pneumoconiosis: analytical scanning electron microscopy and literature review. Mod Pathol. 1995; 8:859–865. Review, 24 refs. [PubMed: 8552576]

Mihara M, Hashizume M, Yoshida H, Suzuki M, Shiina M. IL-6/IL-6 receptor system and its role in physiological and pathological conditions. Clin Sci (Lond). 2012; 122:143–159. [PubMed: 22029668]

Nalabotu SK, Kolli MB, Triest WE, Ma JY, Manne ND, Katta A, et al. Intratracheal instillation of cerium oxide nanoparticles induces hepatic toxicity in male Sprague–Dawley rats. Int J Nanomedicine. 2011; 6:2327–2335. [PubMed: 22072870]

Oyarzun MJ, Clements JA. Control of lung surfactant by ventilation, adrenergic mediators, and prostaglandins in the rabbit. Am Rev Respir Dis. 1978; 117:879–891. [PubMed: 26302]

Pairon JC, Roos F, Iwatsubo Y, Janson X, Billon-Galland MA, Bignon J, et al. Lung retention of cerium in humans. Occup Environ Med. 1994; 51:195–199. [PubMed: 8130849]

Pairon JC, Roos F, Sebastien P, Chamak B, bd-Alsamad I, Bernaudin JF, et al. Biopersistence of cerium in the human respiratory tract and ultrastructural findings. Am J Ind Med. 1995; 27:349–358. [PubMed: 7747741]

Papakonstantinou E, Aletras AJ, Roth M, Tamm M, Karakiulakis G. Hypoxia modulates the effects of transforming growth factor-beta isoforms on matrix-formation by primary human lung fibroblasts. Cytokine. 2003; 24:25–35. [PubMed: 14561488]

Park B, Martin P, Harris C, Guest R, Whittingham A, Jenkinson P, et al. Initial in vitro screening approach to investigate the potential health and environmental hazards of Envirox™ — a nanoparticulate cerium oxide diesel fuel additive. Part Fibre Toxicol. 2007; 4:12. [PubMed: 18053256]

Park EJ, Cho WS, Jeong J, Yi J, Choi K, Park K. Pro-inflammatory and potential allergic responses resulting from B cell activation in mice treated with multi-walled carbon nanotubes by intratracheal instillation. Toxicology. 2009; 259:113–121. [PubMed: 19428951]

Porru S, Placidi D, Quarta C, Sabbioni E, Pietra R, Fortaner S. The potential role of rare earths in the pathogenesis of interstitial lung disease: a case report of movie projectionist as investigated by neutron activation analysis. J Trace Elem Med Biol. 2001; 14:232–236. [PubMed: 11396783]

Sabbioni E, Pietra R, Gaglione P, Vocaturo G, Colombo F, Zanoni M, et al. Long-term occupational risk of rare-earth pneumoconiosis. A case report as investigated by neutron activation analysis. Sci Total Environ. 1982; 26:19–32. [PubMed: 7167813]

Schuetzle D. Sampling of vehicle emissions for chemical analysis and biological testing. Environ Health Perspect. 1983; 47:65–80. [PubMed: 6186484]

Schuetzle D, Lee FS, Prater TJ. The identification of polynuclear aromatic hydrocarbon (PAH) derivatives in mutagenic fractions of diesel particulate extracts. Int J Environ Anal Chem. 1981; 9:93–144. [PubMed: 7012053]

Stone KC, Mercer RR, Gehr P, Stockstill B, Crapo JD. Allometric relationships of cell numbers and size in the mammalian lung. Am J Respir Cell Mol Biol. 1992; 6:235–243. [PubMed: 1540387]

Sulotto F, Romano C, Berra A, Botta GC, Rubino GF, Sabbioni E, et al. Rare-earth pneumoconiosis: a new case. Am J Ind Med. 1986; 9:567–575. [PubMed: 3740074]

Underwood, EE. Quantitative stereology. Addison-Wesley; Reading, MA: 1970.

Vaisman L, Wagner HD, Marom G. The role of surfactants in dispersion of carbon nanotubes. Adv Colloid Interface Sci. 2006; 128–130:37–46.

Valberg PA, Watson AY. Analysis of diesel-exhaust unit-risk estimates derived from animal bioassays. Regul Toxicol Pharmacol. 1996; 24:30–44. [PubMed: 8921544]

Vocaturo G, Colombo F, Zanoni M, Rodi F, Sabbioni E, Pietra R. Human exposure to heavy metals. Rare earth pneumoconiosis in occupational workers. Chest. 1983; 83:780–783. [PubMed: 6839821]

Waring PM, Watling RJ. Rare earth deposits in a deceased movie projectionist. A new case of rare earth pneumoconiosis? Med J Aust. 1990; 153:726–730. [PubMed: 2247001]

Witschi HP, Tryka AF, Lindenschmidt RC. The many faces of an increase in lung collagen. Fundam Appl Toxicol. 1985; 5:240–250. [PubMed: 2580752]

Wynn TA. Fibrotic disease and the T(H)1/T(H)2 paradigm. Nat Rev Immunol. 2004; 4:583–594. [PubMed: 15286725]

Yang HM, Barger MW, Castranova V, Ma JK, Yang JJ, Ma JY. Effects of diesel exhaust particles (DEP), carbon black, and silica on macrophage responses to lipo-polysaccharide: evidence of DEP suppression of macrophage activity. J Toxicol Environ Health. 1999; 58:261–278.

Yang HM, Antonini JM, Barger MW, Butterworth L, Roberts BR, Ma JK, et al. Diesel exhaust particles suppress macrophage function and slow the pulmonary clearance of *Listeria monocytogenes* in rats. Environ Health Perspect. 2001; 109:515–521. [PubMed: 11401764]

Yin XJ, Schafer R, Ma JY, Antonini JM, Weissman DD, Siegel PD, et al. Alteration of pulmonary immunity to *Listeria monocytogenes* by diesel exhaust particles (DEPs). I Effects of DEPs on early pulmonary responses. Environ Health Perspect. 2002; 110:1105–1111. [PubMed: 12417481]

Yin XJ, Schafer R, Ma JY, Antonini JM, Roberts JR, Weissman DN, et al. Alteration of pulmonary immunity to *Listeria monocytogenes* by diesel exhaust particles (DEPs). II Effects of DEPs on T-cell-mediated immune responses in rats. Environ Health Perspect. 2003; 111:524–530. [PubMed: 12676610]

Yin XJ, Dong CC, Ma JY, Antonini JM, Roberts JR, Stanley CF, et al. Suppression of cell-mediated immune responses to listeria infection by repeated exposure to diesel exhaust particles in brown Norway rats. Toxicol Sci. 2004; 77:263–271. [PubMed: 14657513]

Yin XJ, Dong CC, Ma JYC, Antonini JM, Roberts JR, Barger MW, et al. Sustained effect of inhaled diesel exhaust particles on T-lymphocyte-mediated immune responses against *Listeria monocytogenes*. Toxicol Sci. 2005; 88:73–81. [PubMed: 16107554]

Yin XJ, Dong CC, Ma JYC, Roberts JR, Antonini JM, Ma JKH. Suppression of phagocytic and bactericidal functions of rat alveolar macrophages by the organic component of diesel exhaust particles. J Toxicol Environ Health A. 2007; 70:820–828. [PubMed: 17454558]

Yokel RA, Florence RL, Unrine JM, Tseng MT, Graham UM, Wu P, et al. Biodistribution and oxidative stress effects of a systemically-introduced commercial ceria engineered nanomaterial. Nanotoxicology. 2009; 3:234–248.

Yu CP, Yoon KJ. Retention modeling of diesel exhaust particles in rats and humans. Res Rep Health Eff Inst. 1991; 40:1–24. [PubMed: 1716915]

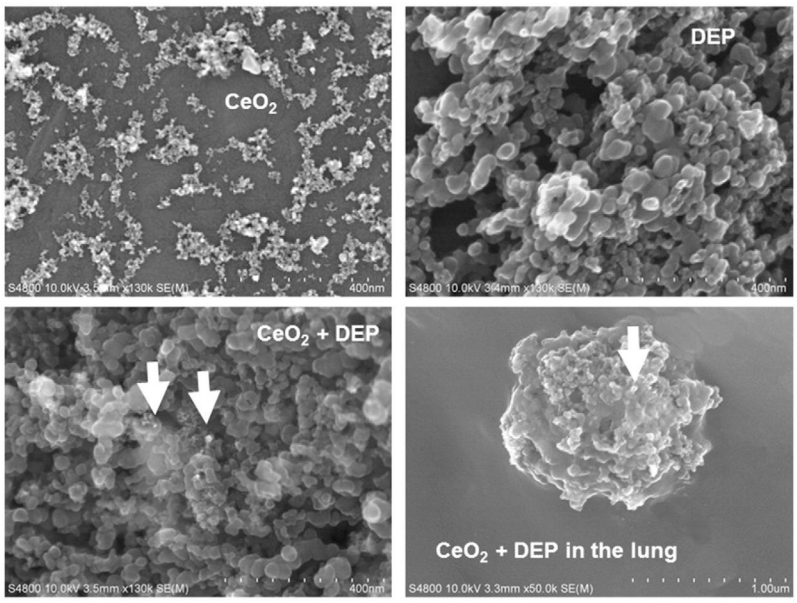

Fig. 1.

Characterization of particle suspensions used for exposure and the presence of DEP and CeO_2 on the epithelial surface in the lung. Field emission SEM of CeO_2, DEP and DEP + CeO_2 nanoparticle suspensions and a DEP + CeO_2 agglomerate on alveolar epithelial surface at 28 days post-exposure (scale bar = 200 nm). $^{+}$Combined exposure is less than DEP alone plus CeO_2 alone, $p < 0.05$.

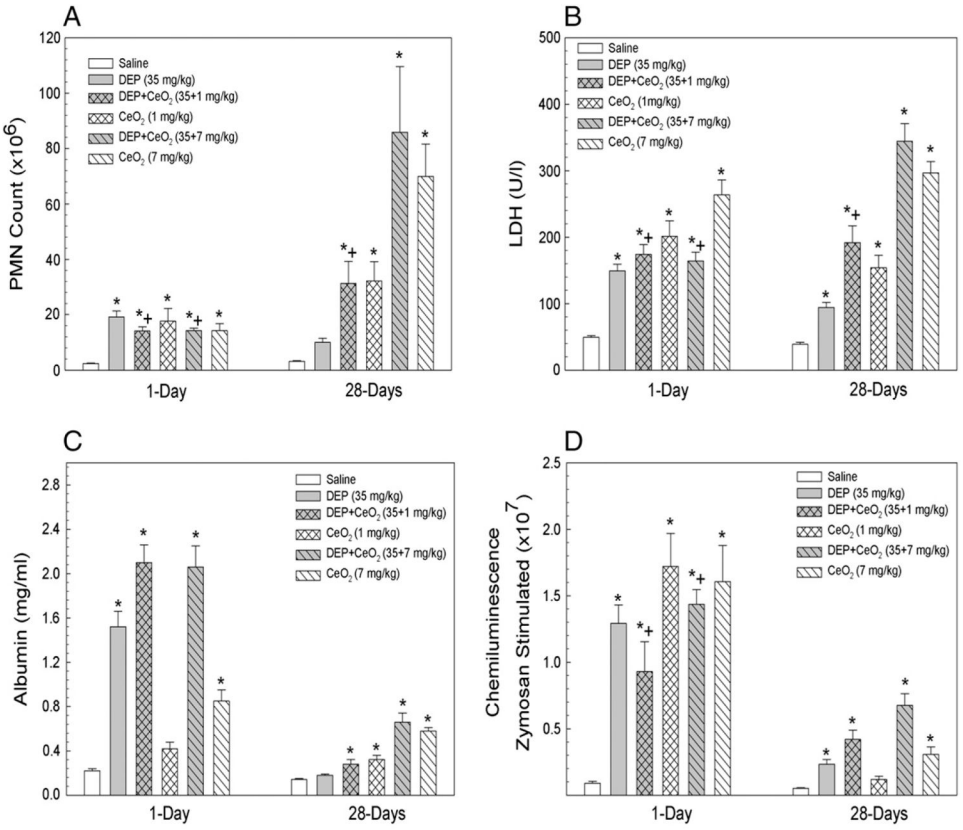

Fig. 2.

Effects of CeO_2 on DEP induced lung inflammation, cytotoxicity, air/capillary damage and ROS generation by AM. Effects of CeO_2 on DEP-induced PMN infiltration, a measure of lung inflammation (A), LDH activity, a marker for the cytotoxicity (B), the amount of albumin in the first lavage fluid, an indicator for the leakage of air/capillary barrier (C), and chemiluminescence generated by AM, a measure of ROS generation (D), are presented. The samples were collected at 1 and 28 days post-exposure. *Significantly different from AM control; $p < 0.05$.

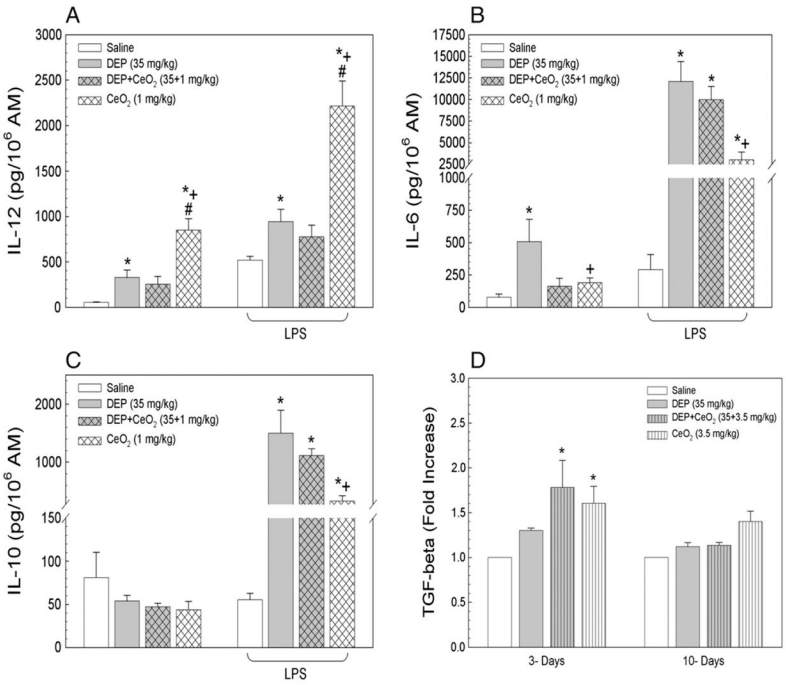

Fig. 3.

Effects of CeO_2 on DEP induced pro- and anti-inflammatory cytokine production by AM with or without ex vivo LPS challenge. AMs were isolated at 1 day after exposure by bronchoalveolar lavage. The productions of IL-12, IL-6 and IL-10 by AM obtained are presented in panels A, B and C, respectively. Panel D shows the production of the fibrotic cytokine, TGF-β1, by AM, isolated at 3 and 10 days post-exposure. *Significantly different from AM control; $p < 0.05$. $^{+}CeO_2$ is significantly different from DEP; $p < 0.05$. $^{\#}CeO_2$ is significantly different from DEP + CeO_2, $p < 0.05$.

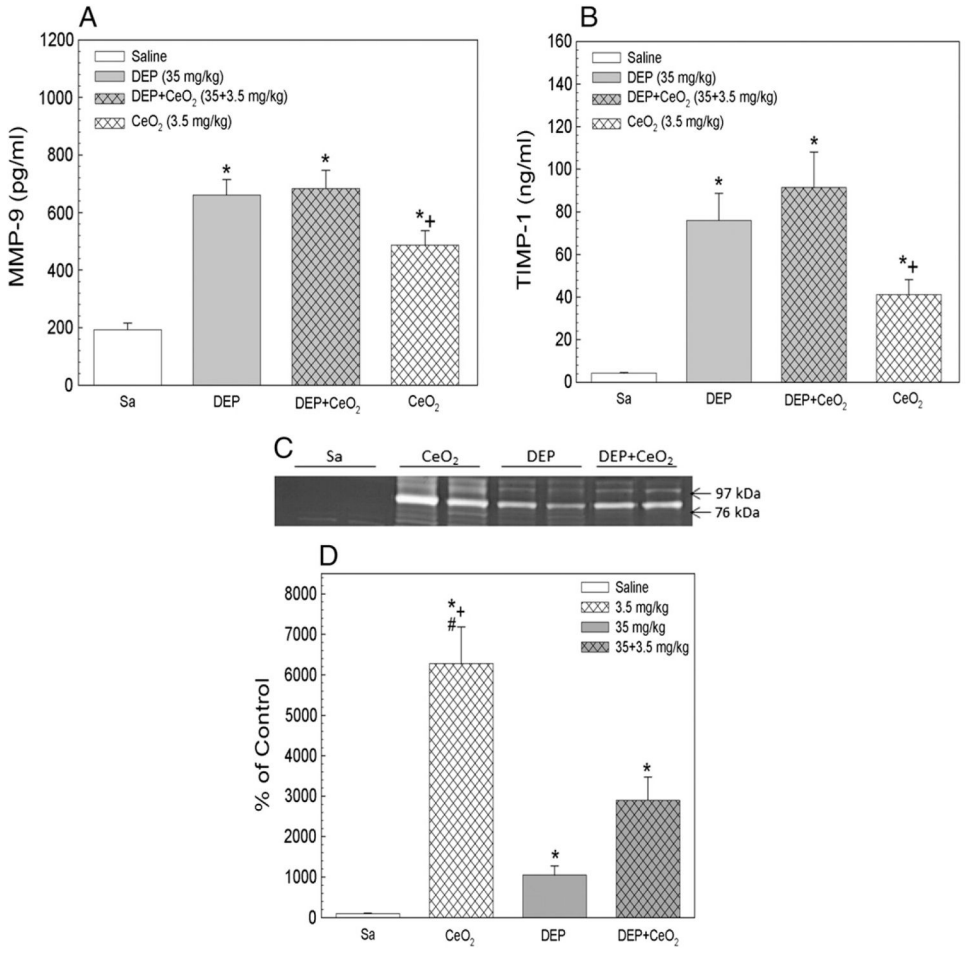

Fig. 4.

Effects of DEP with or without CeO_2 exposure on the induction of MMP-9 and TIMP-1. The protein levels of MMP-9 (A) and TIMP-1 (B) in the first BALF collected at 1 day post-exposure. MMP-9 activity (C and D) in the first BALF from different treatment groups was monitored using Zymography. *Significantly different from control; $p < 0.05$. $^{+}CeO_2$ is significantly different from DEP; $p < 0.05$. $^{\#}CeO_2$ is significantly different from DEP + CeO_2, $p < 0.05$.

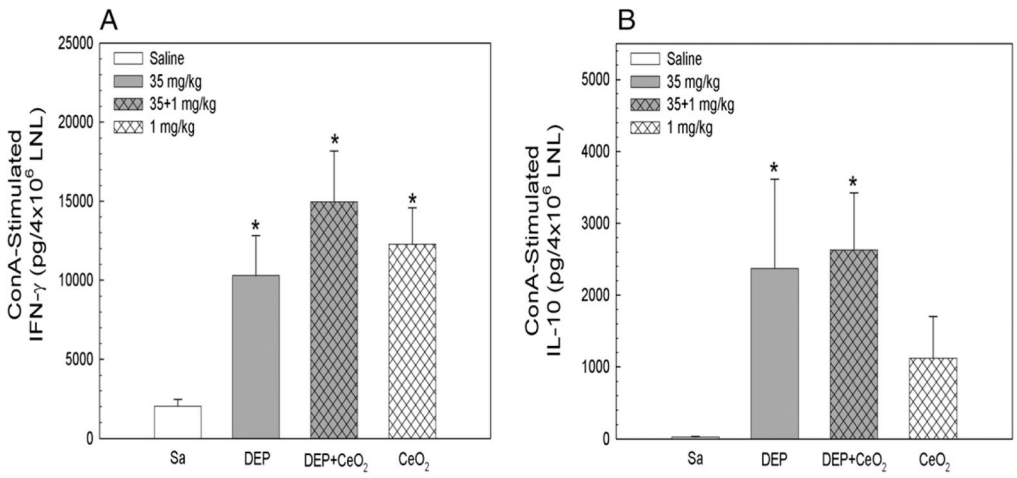

Fig. 5.

Effects of CeO_2 on DEP-induced cytokine production by lymphocytes in response to ConA stimulation. Lymphocytes were isolated at 3 days after exposure. The cytokine IFN-γ and IL-10 productions from lymphocytes obtained at 3 days post-exposure are presented. *Significantly different from control.

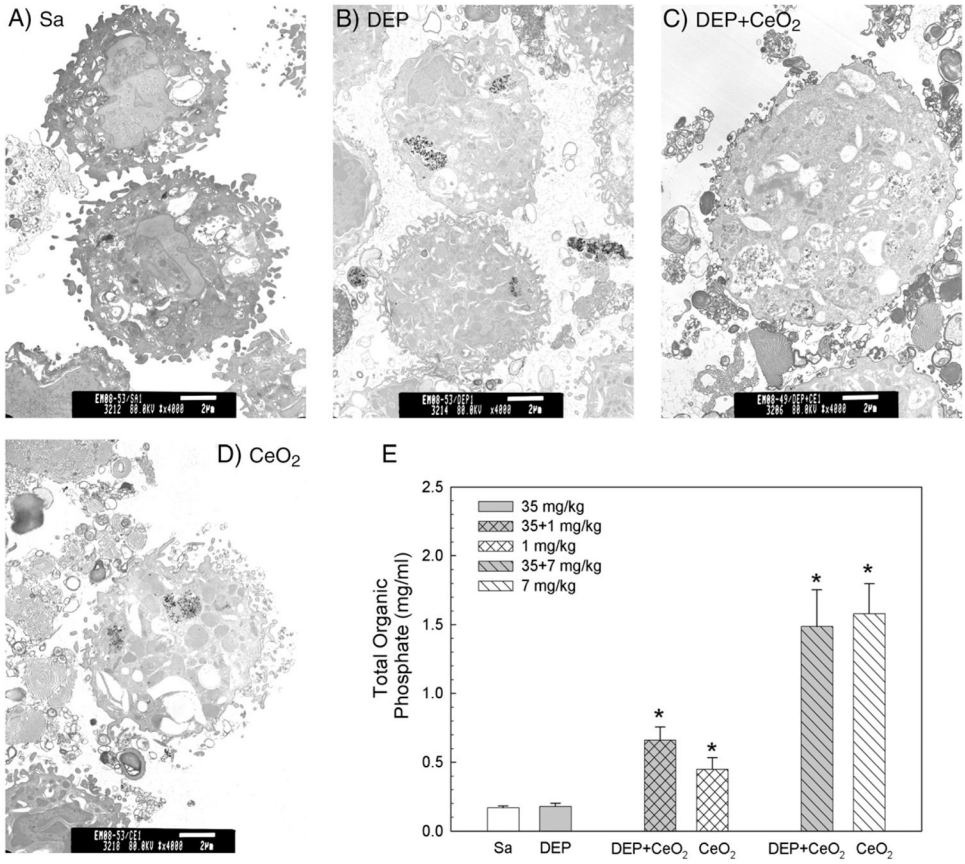

Fig. 6.

Effect of DEP with or without CeO_2 exposure on phospholipid content in the 1st BALF and micrographs of TEM analysis of AM. (A) TEM of AM isolated by bronchoalveolar lavage from (A) control, (B) DEP (35 mg/kg)-, (C) DEP with CeO_2 (3.5 mg/kg)- and (D) CeO_2-exposed rats at 10 days post-exposure (bar = 2 μm). (E) The phospholipid content in the first BALF obtained from saline and various concentrations of CeO_2-exposed rats at 28 days post-exposure. The values are expressed as means ± SE, n = 6. *Significantly different from saline control group at $p < 0.05$.

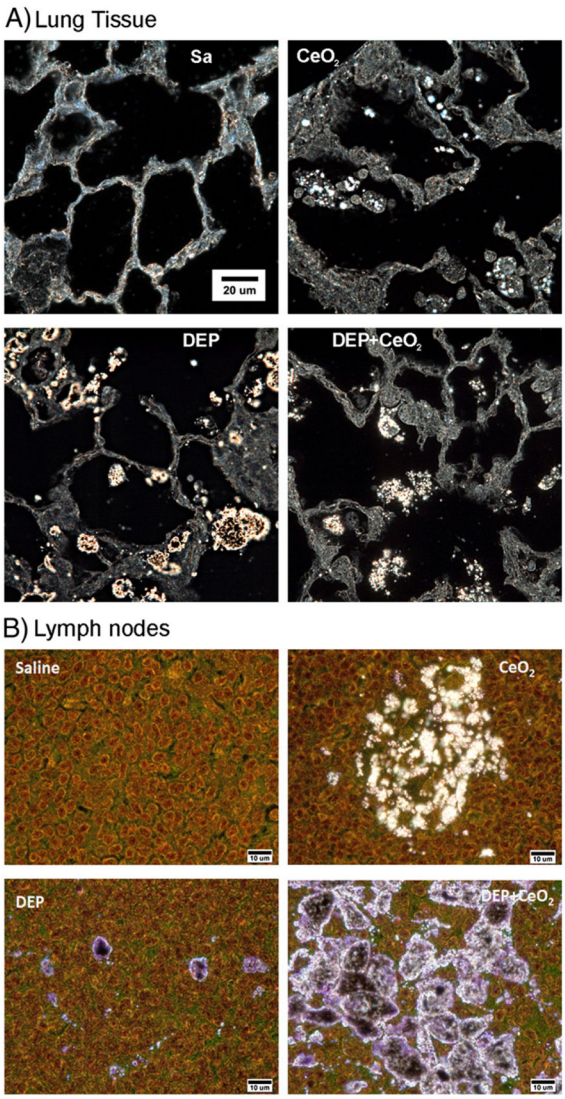

Fig. 7.

CeO_2 particles in the lung tissue and lymph nodes collected from particle-exposed rats, at 28 days post-exposure. Control lung tissues (A) and lymph nodes (B) exhibit no particles under high resolution, dark field illumination. Illuminated CeO_2 particles, using enhanced darkfield-based illumination, were clearly detected in the macrophages, in the interstitium, in the acellular surfactant clumps, and in the airspace of the CeO_2 (7 mg/kg)- and DEP (35 mg/kg) + CeO_2-exposed lungs at 28 days after exposure. As shown in the representative micrographs, lymph nodes of CeO_2-exposed lungs contained isolated clusters of particle accumulations. Lymph nodes of DEP-exposed lungs demonstrated isolated, dense clumps of particles, while the combined exposure (CeO_2 + DEP) resulted in nearly continuous particle accumulations throughout the lymph node.

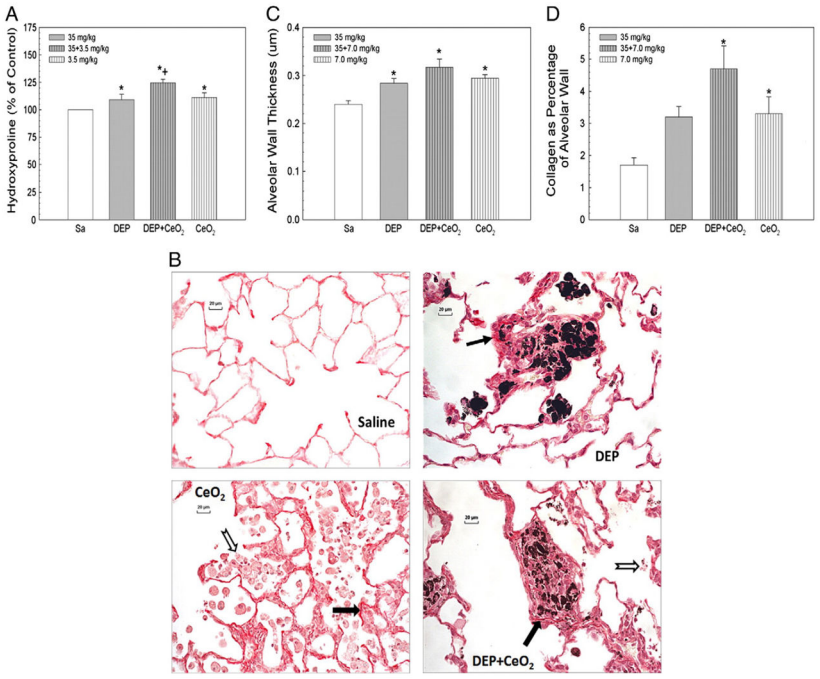

Fig. 8.

Effects of DEP-, CeO_2- and DEP + CeO_2-exposure on hydroxyproline content and Sirius Red staining for collagen in the lung tissue and quantitative morphometric analysis of alveolar wall thickness and alveolar collagen fiber volume in rat lung tissues. (A) Hydroxyproline content in the lung tissue. The values are expressed as means ± SE, n = 6. (B) Light micrograph of Sirius Red staining for collagen formation in the lung tissues (arrow) at 28 days post-exposure (cerium dose: 7 mg/kg). Acellular surfactant clumps (open arrow) were detected in the airspace of the CeO_2 (7 mg/kg)- and DEP (35 mg/kg) + CeO_2-exposed lungs. (C) Quantitative analysis of dose-dependent increase in the thickness of alveolar wall connective tissue. (D) Quantitative analysis of alveolar collagen volume expressed as a percentage of total tissue volume, based on the morphometric analysis of Sirius Red stained sections. *Significantly different from saline controls; $p < 0.05$. $^{+}$Significantly different from CeO_2 alone or DEP alone groups, at $p < 0.05$.

Table 1

Effects of DEP, CeO_2 and DEP + CeO_2 on lymphocyte differentiation in LDL at 28 days post-exposure.

Particle dose (mg/kg)	Lymphocytes (×10^6)	T cells (×10^6)	$CD4^+$ T cells (×10^6)	$CD8^+$ T cells (×10^6)	$CD4^+/CD8^+$	B220 (×10^6)	NK (×10^6)	NKT (×10^6)
Saline	24.67 ± 2.58	14.45 ± 1.35	8.52 ± 0.84	5.02 ± 0.55	1.73 ± 0.988	9.34 ± 1.19	.276 ± 0.54	.32 ± 0.070
DEP (35.0)	94.64 ± 7.88*	57.36 ± 4.78*	29.50 ± 2.57*	23.11 ± 2.08*	1.28 ± 0.062*	33.93 ± 3.53*	.753 ± 0.081*	1.26 ± 0.0876*
CeO_2 (1.0)	56.58 ± 2.94*	33.36 ± 1.71*	16.62 ± 0.93*	13.97 ± 0.82*	1.21 ± 0.062*	21.45 ± 1.99*	.482 ± 0.0546	.85 ± 0.080*
DEP + CeO_2 (35.0 + 1.0)	104.57 ± 9.633	65.46 ± 6.43*	34.79 ± 3.16*	27.44 ± 2.69*	1.27 ± 0.329*	35.80 ± 3.33*	.966 ± 0.1106*	1.44 ± 0.211*

Values are expressed as mean ± SE (n = 6). Data were analyzed by one-way ANOVA with means testing by Dunnett's test to compare treatment groups to control for multiple mean comparisons for each treatment. The viability of all cell preparations was above 98%.

*Significantly different from the saline controls, $p < 0.05$.